





Modeling the limiting performance of resistive superconductor fault current limiters for 2G HTS tape

Rezistif süperiletken arıza akımı sınırlayıcıların sınırlandırma performansının 2G HTS şerit için modellenmesi

Buğra YILMAZ^{1*} , Muhsin Tunay GENÇOĞLU² 

^{1,2}Department of Electrical-Electronics Engineering, Faculty of Engineering, Firat University, Elazığ, Turkey.

¹b.yilmaz@firat.edu.tr, ²mtgencoglu@firat.edu.tr

Received: 14.04.2022
Accepted: 06.05.2022

Revision: 28.04.2022

doi: 10.5505/fujece.2022.32042
Research Article

Abstract

Fault currents in power systems force valuable power system elements thermally, electro-dynamically and electromagnetically. Due to the increase in fault current levels, the installation of components resistant to fault currents and the damage of these currents to existing components bring economic problems. Therefore, various modern limiting methods have been developed in recent years. One of these methods, Resistive Superconducting Fault Current Limiter (R-SFCL), increases the security and sustainability of the system by eliminating these risks. This study made a dynamic model in MATLAB/Simulink by creating a sample R-SFCL in the laboratory using a 2G HTS (High-Temperature Superconductor) tape. With this model, the limitation analysis for single phase-ground fault is observed. The simulation results and the responses of the sample R-SFCL were compared and it was concluded that they showed a great deal of similarity.

Keywords: 2G HTS tape, Fault current limiting, Resistive SFCL, Simulation, Design.

Özet

Güç sistemlerindeki arıza akımları, değerli güç sistemi elemanlarını termal, elektro dinamik ve elektromanyetik olarak zorlamaktadır. Arıza akım seviyelerinin yükselmesi sebebiyle hem arıza akımlarına dayanıklı bileşenlerin tesisi hem de bu akımların mevcut bileşenlere zarar vermesi ekonomik problemleri beraberinde getirmektedir. Son yıllarda çeşitli modern sınırlandırma yöntemi geliştirilmiştir. Bu yöntemlerinden biri olan Rezistif Süperiletken Arıza Akım Sınırlayıcı (R-SFCL), bu riskleri ortadan kaldırarak sistemin güvenliğini ve sürdürülebilirliğini artırmaktadır. Bu çalışmada, 2G HTS (Yüksek Sıcaklıklı Süperiletken) şerit kullanılarak laboratuvar ortamında örnek bir R-SFCL oluşturularak MATLAB/Simulink'te dinamik bir modeli yapılmıştır. Bu model ile tek faz-toprak arızası için sınırlandırma analizi gözlemlenmiştir. Simülasyon sonuçları ile örnek R-SFCL'nin gösterdiği tepkiler karşılaştırılmış ve büyük oranda benzerlik gösterdikleri sonucuna varılmıştır.

Anahtar kelimeler: 2G HTS şerit, Arıza akımı sınırlandırma, Rezistif SFCL, Simülasyon, Tasarım.

1. Introduction

Increasing world population and industrialization have led to increased energy demand. New electricity generation, transmission and distribution systems are added to existing systems to meet the increasing demand for electrical energy. The increase in production capacity also increases the level of short-circuit currents. High-level fault currents can cause irreversible damage to power system elements. Therefore, power system breakers need to trip the fault current as soon as possible. Considering that the tripping capacity of typical high voltage breakers is limited to 80 kA, increased fault current levels will quickly exceed the capabilities of existing breakers [1]. Higher tripping capacity increases both the size and cost of breakers. Because of these situations, it is necessary to reduce the fault current quickly to non-hazardous levels. Many methods have been developed in recent years to limit the current. The series reactors added to the circuit limit the current, but they cause high voltage drop and power loss under normal operating conditions. While fuses called is-limiters do not cause power loss under normal conditions, they have the disadvantage of replacing the fuse after each short circuit

*Corresponding author

[2]. Superconducting Fault Current Limiters (SFCL), one of the modern fault current limiting methods, are a good solution for fault currents [3]. Elimination of fault currents and hazards is possible using SFCLs, which use the abrupt transition of superconducting material from the superconductor to the resistive region at a given critical current value [4]. SFCL causes low voltage drop and power loss at rated current. If critical values such as critical temperature (T_c), critical current density (J_c) and critical magnetic field (H_c) are exceeded, the resistance of the superconductor will increase [5].

After the short circuit is over, the SFCL cools down and returns to the superconducting region. SFCL can usually be isolated from the system during cooling by a circuit breaker [6]. SFCL can be classified into two different types in practice. These are Resistive SFCL and Inductive SFCL. R-SFCL is the ideal type due to its small size and reduced price of superconductors [7]. At the same time, R-SFCL reduces the effect of the DC factor of the fault current by lowering the X/R ratio and makes the breakers' work easier. It does not generate harmonics and does not cause magnetic field interference. R-SFCL applications in power systems have recently been preferred thanks to these advantages. Many superconducting materials are used in the R-SFCL design. These materials are divided into two groups according to their temperature: High-Temperature Superconductors (HTS) and Low-Temperature Superconductors (LTS). The HTS is cooled with liquid Nitrogen (LN_2) and has a critical temperature of over 30°K. This is a massive advantage over LTS materials, which operate at 4.2 °K, are very close to their critical temperature and are very sensitive to temperature changes. SFCL based on LTS has not been widely used as it requires a costly cooling system using liquid Helium (LHe) [8]. However, when using HTS for SFCL applications, cooling costs can be reduced ten times than LTS [9].

HTS materials are also divided into two groups 1G and 2G. 2G HTS materials have higher current carrying capacity, critical current level, magnetic flux value and mechanical strength. In addition, 2G materials pass into the resistive region faster than 1G materials [10]. Similarly, after the fault is complete, the 1G HTS returns to the superconducting region later than the 2G HTS. The 1G HTS has a lower normal operating resistance than the 2G HTS [11]. In brief, 2G HTS is an ideal choice for R-SFCL due to its high linear resistances, high current density and ability to operate in liquid nitrogen with low cryogenic costs [12]. In this paper, a sample R-SFCL application was created using 2G HTS tape in the laboratory, a dynamic model was developed in MATLAB/Simulink and the limitation analysis of 2G HTS materials was examined.

2. Materials and Method

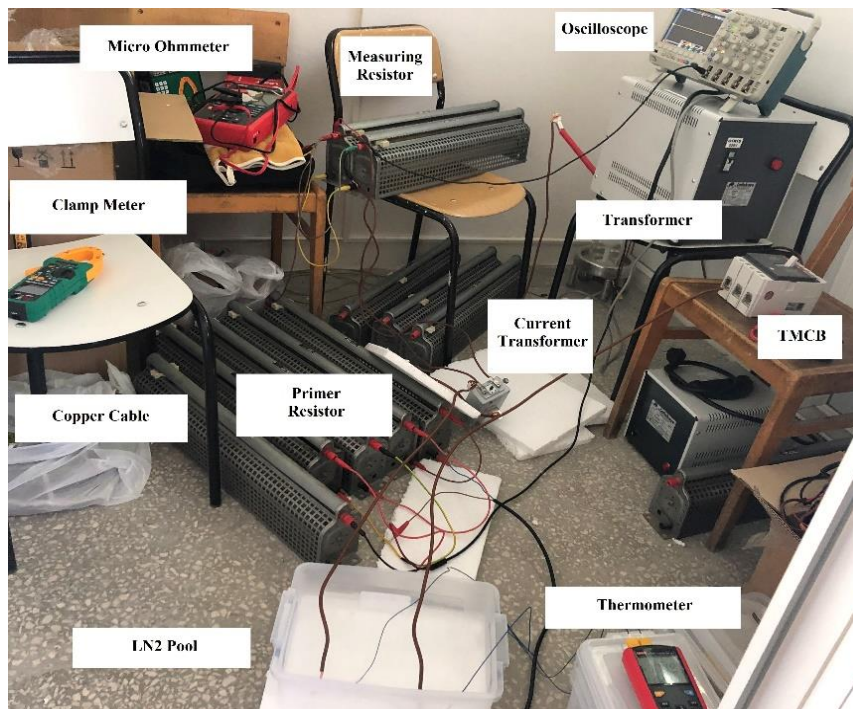
The system elements on which the tests were tested and the measurements were made are given in Table 1. To create the sample R-SFCL, a 2 m long 2G HTS tape produced by SuperPower company was divided into 40 cm lengths. The thickness of the superconducting tape is 6 mm and its critical current is 180 A. Details about the superconducting tape are given in Appendix A.

Table 1. System elements

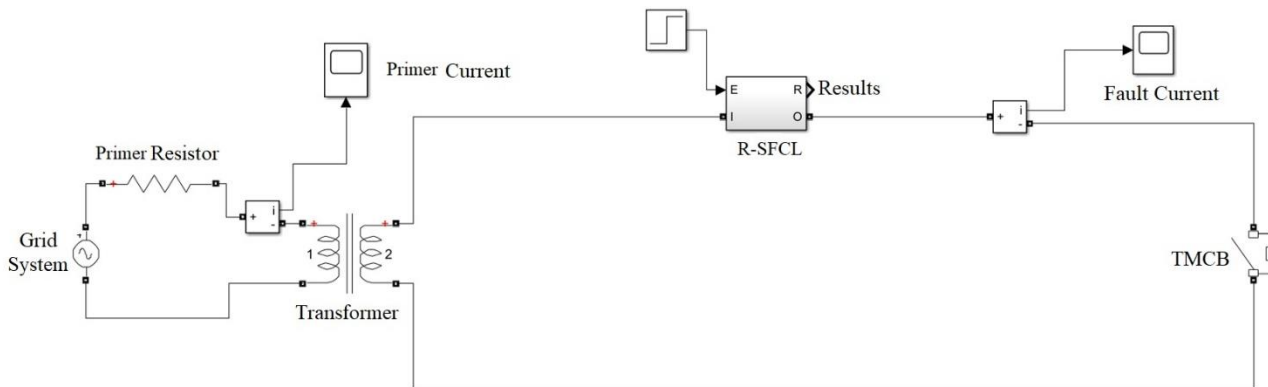
Element	Specification
Transformer	3 kVA, 220/5 V
Current Transformer	500/5 A
Thermal Magnetic Circuit Breaker (TMCB)	250 A
Primer Resistor	21.39 Ω
Measuring Resistor	1 Ω
Clamp Meter	USB Connected
Micro Ohmmeter	USB Connected
Thermometer	K Type Thermocouple USB Connected

Connections in the system were made with copper cable with a cross-section of 10 mm². The instantaneous short circuit current of the cable is 1 kA and its insulator is PVC. Since short circuit tests are carried out, the insulator must be resistant to high temperatures. The cable insulator used is temperature resistant up to 180 °C.

R-SFCL's LN₂ pool with a 6-liter plastic container. The container is soft plastic so that it does not crack in contact with LN₂. In addition, LN₂ was stored in a particular 10-liter cryogenic container. The overview of the test system is in Figure 1(a) and the Simulink model is shown in Figure 1(b).



(a)



(b)

Figure 1. (a) Test system (b) Simulink model

The current waveforms in the experiments were obtained by observing the voltage on the 1 Ω resistor on the oscilloscope screen. The current was also recorded instantaneously as an effective value with the help of a clamp meter. The temperature change of the superconductor during the failure was also instantly transferred to the computer with a K-type thermocouple thermometer. Superconducting tapes are soldered to one end of the copper plates to provide better transition resistance. Cable ends are connected to the other end of the copper plates. The fault was carried out with TMCB and 250 A was chosen to avoid damage to the superconducting tape. The superconductor connection with the copper plate is shown in Figure 2.



Figure 2. Superconducting tape connection with copper plate

2.1. Modeling

The current through the R-SFCL is less than the critical current value during normal operating conditions. Therefore, the resistance is close to zero and the R-SFCL conducts electricity almost without loss. However, in the event of a fault, the current exceeds the critical current value and the resistance of the superconducting material increases. Thus, the R-SFCL limits the fault current [13]. Briefly, R-SFCL, which produces a negligible voltage drop and power loss in normal operation, limits the fault current level with a nonlinear increase in resistance within the first half-period when the fault occurs.

R-SFCL model and simulations were performed in MATLAB-Simulink. The E-J curve of the superconducting material is based on the modeling [14-16]. In the R-SFCL model created in Simulink, the effective value of the system current is compared with the critical current value of the 2G HTS tape at any time. According to the E-J curve, there are three regions for the superconducting material: superconductivity, flux-flow and resistive. This curve is given in Figure 3. The resistance of R-SFCL for all three regions was calculated instantaneously by Equation 1. The current density was calculated by Equation 2.

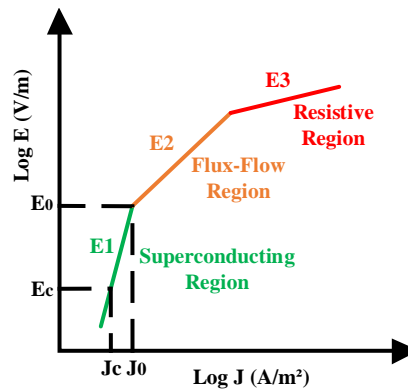


Figure 3. The E-J curve

$$R_{R-SFCL}(t) = \frac{E(J,T) \cdot L_s}{J(t) \cdot A_s} \quad (1)$$

$$J(t) = \frac{I_{R-SFCL}(t)}{A_s} \quad (2)$$

where, R_{Rsfcl} is the instant R-SFCL resistance (Ω), L_s is the superconductor length (m), A_s is the superconductor section (m^2), E is the electric field as a function of J and T (V/m), T is the instant R-SFCL temperature ($^{\circ}K$), I_{Rsfcl} is the instant R-SFCL current (A) and J is the instant current density (A/m^2).

2.2. Superconducting region

The R-SFCL current is below the critical value and the R-SFCL resistance is theoretically zero. E is calculated by Equation 3 [17-20].

$$E(J, T) = E_c \left(\frac{J}{J_c(T)} \right)^\alpha \quad (3)$$

$$J_c(T) = J_c \left(\frac{T_c - T}{T_c - T_0} \right) \quad (4)$$

$$\alpha_x = \frac{\log(E_0/E_c)}{\log \left((J_c/J_c(T))^{(1-\frac{1}{\beta})} (E_0/E_c)^{\frac{1}{\alpha}} \right)} \quad (5)$$

$$\alpha = \max[\beta, \alpha_x] \quad (6)$$

where, E_c is the critical electric field (1 $\mu\text{V}/\text{cm}$), $J_c(T)$ is the critical current density (A/m^2) as a function of T , J_c is the critical current density at 77 °K, T_c is the critical temperature (°K), T_0 is the first temperature value (77 °K), α_x is the time-varying value of the exponential value, α is the superconducting region exponent value, the α value ranges from 5-15 for 1G HTS materials and 15-40 for 2G HTS materials [19], [21], [22].

2.3. Flux-flow region

Exceeding the critical current increases the R-SFCL resistance as the electric field increases and the current is limited. The temperature rises and the rising temperature lowers $J_c(T)$, so the electric field increases continuously. E is calculated by Equation 7 [5, 18, 23].

$$E(J, T) = E_0 \cdot \left(E_c/E_0 \right)^{\beta/\alpha} \frac{J_c}{J_c(T)} \left(J/J_c \right)^\beta \quad (7)$$

where, E_0 is the electric field during the transition from the superconducting region to the flux-flow region (V/m) and takes a value between 0.1 and 1 V/m , β is the exponent of the flux-flow region, for both 1G and 2G HTS materials range from 2-4 [19], [21], [22].

2.4. Resistive region

As soon as the temperature exceeds the critical temperature, R-SFCL is no longer superconducting. R-SFCL resistance and E vary with J and T . E is calculated by Equation 8 [5, 18, 23].

$$E(J, T) = \rho(T_c) J \frac{T}{T_c} \quad (8)$$

where, $\rho(T_c)$ is the superconductor resistivity in the resistive region ($\Omega \cdot \text{m}$).

During this process, the superconducting material heats up. After a recovery time, the cryogenic system cools the superconducting material and returns to the R-SFCL superconducting region. There is continuous heat transfer between the LN_2 and the superconducting tape during and after the limiting process. The heat transfers between LN_2 and superconducting material and R-SFCL temperature change were calculated with Equations 9, 10, 11, 12 and 13, respectively [5, 17, 18, 23-26].

$$Q_{Rsfcl}(t) = \int I_{Rsfcl}(t)^2 R_{Rsfcl}(t) dt \quad (9)$$

$$Q_{cryosys}(t) = \int \left(\frac{T(t)-T_0}{\theta_s} \right) dt \quad (10)$$

$$\theta_s = \frac{1}{k L_s \pi d_s} \quad (11)$$

$$T_{Rsfcl} = T_{Rsfcl} + (Q_{Rsfcl} - Q_{cryosys})/c_s \quad (12)$$

$$c_s = L_s A_s c_{vol} \quad (13)$$

where, Q_{Rsfcl} is the heat energy emitted by the R-SFCL (J), $Q_{cryosys}$ is the heat energy received by the cryogenic system (J), θ_s is the thermal resistance between R-SFCL and cryogenic system (K/W), k is the heat transfer coefficient to the cryogenic system (W/Km²), d_s is the superconductor diameter (m), c_s is the superconductor heat capacity (J/K), c_{vol} is the superconductor volumetric specific heat (J/Km³), T_{Rsfcl} is the R-SFCL instant temperature (°K).

All equations were created as M-function in Simulink according to the algorithm flow chart in Figure 4.

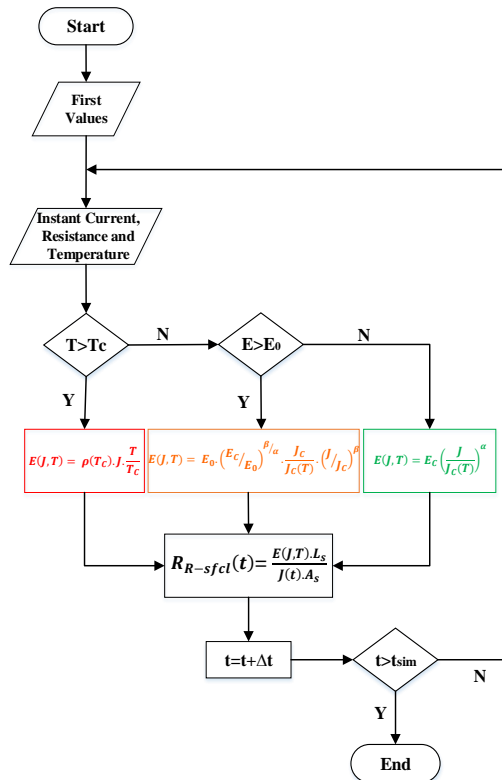


Figure 4. The algorithm flow chart

3. Results

This section observed R-SFCL responses with a fault current of 189 A_{rms}. At the same time, the same fault situation was simulated in the model that created it and the results were examined. A short circuit current of 189 Arms was provided with a primary resistance of 21.39 Ω added to the transformer primary to perform the limitation analysis. First of all, the

fault current was observed for the absence of R-SFCL in the experimental system. Figure 5 shows the fault current waveform measured over a 500/5 A current transformer and a 1 Ω measuring resistor. Figure 6 also shows the fault current with R-SFCL.



Figure 5. Fault current in the system without R-SFCL

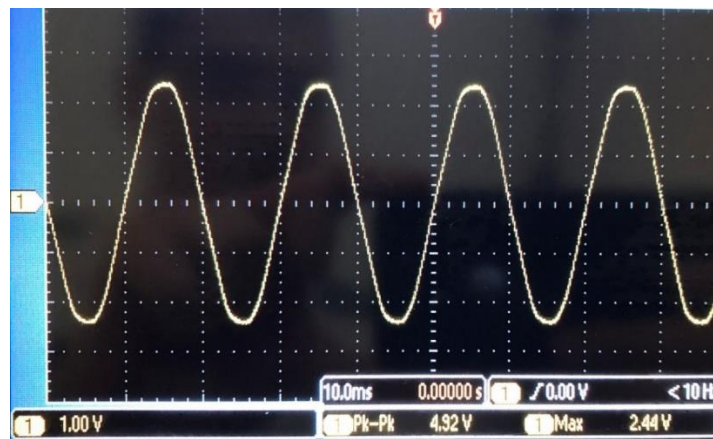


Figure 6. Fault current in the system with R-SFCL

As seen in Figure 5, the peak value of the current was 2.6 A. Since the current transformer ratio is 100, the real peak value of the fault current in the system without R-SFCL was 260 A. When R-SFCL, which used only 40 cm 2G HTS tape, was added to the system for the same fault, the real peak value became 244 A and decreased by 16 A.

In the simulations performed with the model created in MATLAB/Simulink, the fault currents for the system without R-SFCL and with R-SFCL were shown in Figures 7 and 8, respectively.

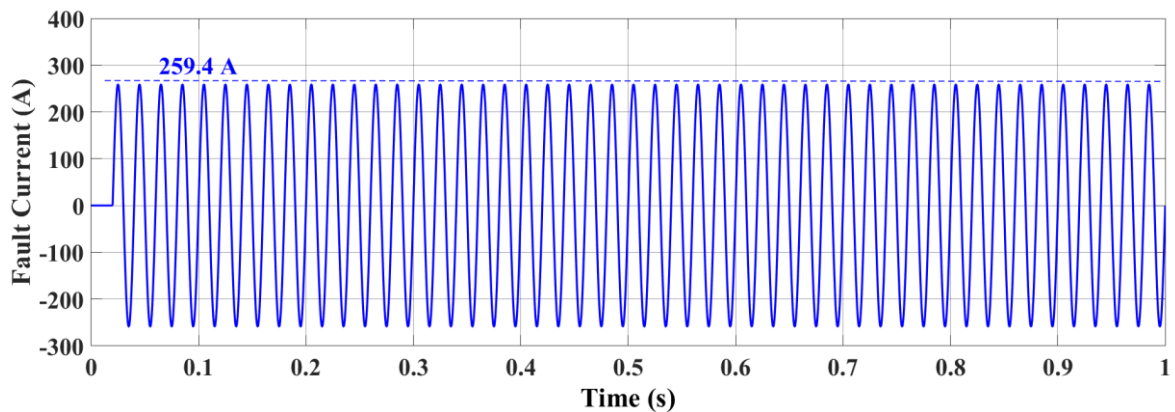


Figure 7. Fault current in the system without R-SFCL

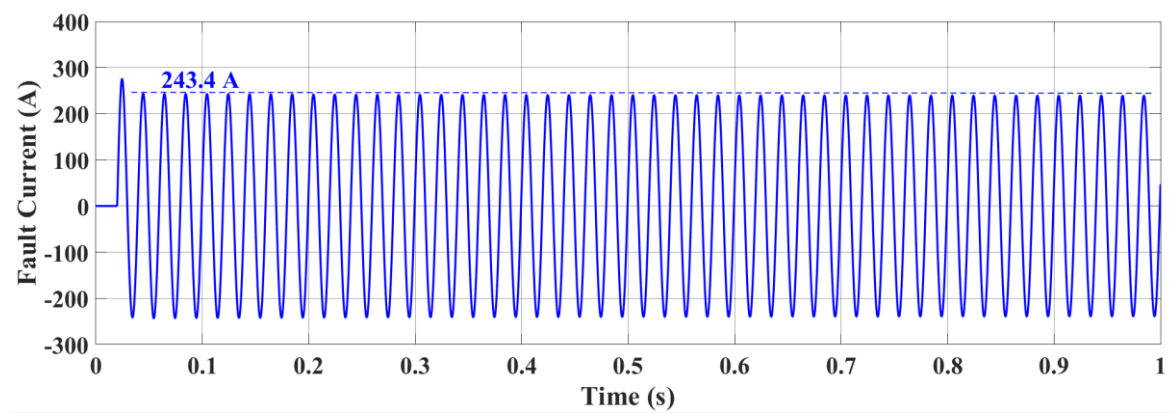


Figure 8. Fault current in the system with R-SFCL

As seen in the simulation results, the peak values of the fault current for both the case without R-SFCL and with R-SFCL were close and consistent with the test results. From the voltage and current data measured during the fault, it has been seen that the fault resistance varies between $7 \text{ m}\Omega$ and $7.1 \text{ m}\Omega$. While the nominal resistance of the tape was $876.404 \mu\Omega$, it increased approximately 8.1 times with the fault. Finally, the resistance change observed in the model created is shown in Figure 9 and it is quite close to the experimental result.

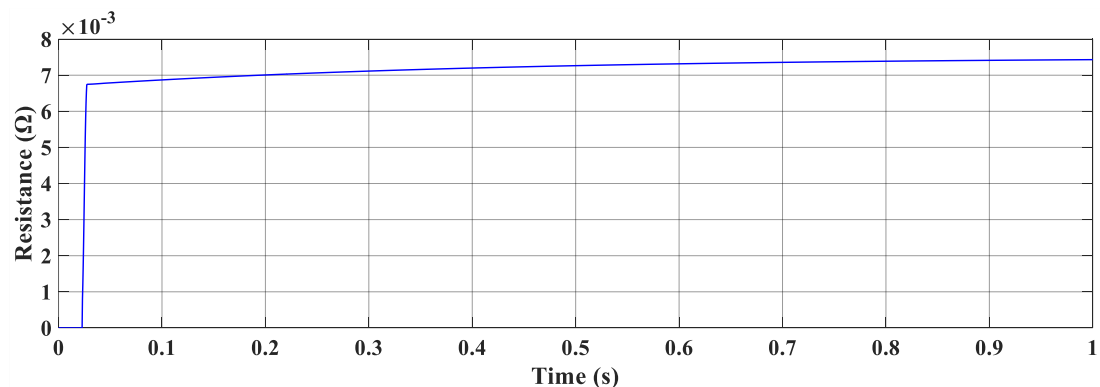


Figure 9. R-SFCL resistance

The rapidly increasing resistance value at the time of fault also caused an increased temperature and the temperatures at the points where the K-type thermocouple terminals were connected varied between $77\text{-}340 \text{ }^\circ\text{K}$. After reaching these

temperature values, the tape must be cooled quickly and effectively. As a matter of fact, in some experiments, the superconducting tapes were damaged and burned. Examples of damaged superconducting tapes are shown in Figure 10.



Figure 10. Damaged superconducting tapes

The reason for this situation is the Hot-Spot event. Hot-Spot is due to the inhomogeneity of the critical current distribution on the tape surface. The tapes were irreversibly damaged as a result of the Hot-Spot. Manufacturers and developers use the thick silver layer and Hastelloy C276 layer throughout the superconducting material to solve this problem [27]. With the addition of these layers with high resistive properties, the thermal mass of the superconducting tape, whose linear resistance decreases, will increase [28]. Other ways to circumvent the Hot-Spot issue are still in development today. One is to use a sapphire-based substrate, while the other is to change the architecture of the tape. A closed-loop cooling system will also minimize the possibility of Hot-Spot occurrence. In this study, since it is an open-loop cooling system, the occurrence of Hot-Spot was inevitable according to the fault time and current level. At the same time, the cable-connected parts of the copper plates that are soldered to the strips remain outside the liquid nitrogen. This part, which is directly at room temperature, also causes rapid evaporation of liquid nitrogen. This situation is similar to current leads in real R-SFCL applications. The current leads are one of the R-SFCL's most significant design issues because they directly reduce the cooling capacity.

4. Conclusions

In this study, a laboratory sample of R-SFCL used a 40 cm long 2G HTS tape was made and this sample was modeled in MATLAB/Simulink. Experiment and simulation results were compatible with each other and R-SFCL reduced the peak value of fault current by 16 A. This tape, which causes negligible power loss and voltage drop by showing resistance of about $880 \mu\Omega$ in the nominal operating condition, limited the fault by showing resistance of $7 \text{ m}\Omega$ during the fault. Future studies will examine the effects of winding shapes on efficiency and limitation analyses by supplying longer tapes.

5. Acknowledgments

This study was supported by Firat University Scientific Research Foundation (Project Numbers MF.20.02).

6. Author Contribution Statement

In this study, Author 1 contributed to the creation of the idea, the design and the literature review, the evaluation of the results obtained, the procurement of the materials used and the analysis of the results; Author 2 contributed to the creation of the idea, spelling, the procurement of the materials used, reviewing the results and checking the paper for content.

7. Ethics Committee Approval and Conflict of Interest

There is no need for an ethics committee approval in the prepared article. There is no conflict of interest with any person/institution in the prepared article.

8. References

- [1] Seyedi H, Tabei B. “Appropriate placement of fault current limiting reactors in different hv substation arrangements”. *Circuits Syst.*, 03, 03, 252–262, 2012.
- [2] Kempinski A, Rusinski J, Hajdasz S. “Analysis of Recovery Time of HTS tapes with electrical insulation layers for superconducting fault current limiters under load conditions”. *IEEE Trans. Appl. Supercond.*, 29, 8, 2019.
- [3] Blair SM, Booth CD, Burt GM. “Current-time characteristics of resistive superconducting fault current limiters”. *IEEE Trans. Appl. Supercond.*, 22, 2, 2012.
- [4] M. C. Nagarathna V. M. H. and S. R., “A Review on Super Conducting Fault Current Limiter (SFCL) in power system,” 3, 2, 485–489, 2015.
- [5] Zhang X, Ruiz HS, Zhong Z, Coombs TA. “Implementation of resistive type superconducting fault current limiters in electrical grids : performance analysis and measuring of optimal locations”. *Superconductivity*, 4, 1-6, 2015.
- [6] Gorbunova DA, Kumarov DR, Scherbakov VI, Sim K, Hwang S. “Influence of polymer coating on SFCL recovery under load”. *Prog. Supercond. Cryog.*, 12, 1, 44–47, 2020.
- [7] Zhu J, Zhao Y, Chen P, Gong J, Jiang S, Wang S. “Performance analysis on a flux coupling superconducting fault current limiter (SFCL) considering the power grid integration based on MATLAB / SIMULINK”. *2018 IEEE Int. Conf. Appl. Supercond. Electromagn. Devices*, 3, 1–2, 2018.
- [8] Ignatius OK. “Transient stability improvement using resistive-type superconducting fault current limiters (R-SFCL)”. *Int. J. Eng. Technol. Sci.*, 6, 2, 28–41, 2019.
- [9] Zenitani Y, Akimitsu J. “Discovery of the new superconductor MgB₂ and its recent development”. *Oyobuturi*, 71, 1, 17–22, 20027.
- [10] Kim JS, Lim SH, Kim JC. “Study on application method of superconducting fault current limiter for protection coordination of protective devices in a power distribution system”. *IEEE Trans. Appl. Supercond.*, 22, 3, 4–7, 2012.
- [11] Kulkarni S, Dixit M, Pal K. “Study on recovery performance of high T_c superconducting tapes for resistive type superconducting fault current limiter applications”. 36, 1231–1235, 2012.
- [12] Zampa A, Holleis S, Badel A, Tixador P, Bernardi J, Eisterer M. “Influence of local inhomogeneities in the REBCO layer on the mechanism of quench onset in 2G HTS Tapes”. *IEEE Trans. Appl. Supercond.*, 32, 3, 2022.
- [13] Moyzykh M. *et al.* “First Russian 220 kV superconducting fault current limiter for application in city grid”. *IEEE Trans. Appl. Supercond.*, 31, 5, 1–7, 2021.
- [14] Hatata AY, Ebeid AS, El-Saadawi MM. “Application of resistive super conductor fault current limiter for protection of grid-connected DGs”. *Alexandria Eng. J.*, 57, 4, 4229–4241, 2018.
- [15] De Sousa WTB, Polasek A, Dias R, Matt CFT, De Andrade R. “Thermal-electrical analogy for simulations of superconducting fault current limiters”. *Cryogenics (Guildf)*, 62, 97–109, 2014.
- [16] Chen Y, Li S, Sheng J, Jin Z, Hong Z, Gu J. “Experimental and numerical study of co-ordination of resistive-type superconductor fault current limiter and relay protection”. *J. Supercond. Nov. Magn.*, 26, 11, 3225–3230, 2013.
- [17] Blair S.M, Booth CD, Burt GM. “Current-time characteristics of resistive superconducting fault current limiters”. *IEEE Trans. Appl. Supercond.*, 22, 2, 5600205, 2012.
- [18] Nemdili S, Belkhiat S. “Modeling and simulation of resistive superconducting fault-current limiters”. *J. Supercond. Nov. Magn.*, 25, 7, 2351–2356, 2012.
- [19] Dutta S, Babu BC. “Modelling and analysis of resistive Superconducting Fault Current Limiter”. *IEEE TechSym 2014 - 2014 IEEE Students’ Technol. Symp.*, 362–366, 2014.
- [20] Liang H, Chen Y, Duan R, Lu Y, Sheng J. “Numerical Study on the on-grid performance of superconducting cable cooperated with R-SFCL”. *IEEE Trans. Appl. Supercond.*, 32, 4, 2022.
- [21] Qian K, Guo Z, Terao Y, Ohsaki H. “Electromagnetic and thermal design of superconducting fault current limiters for DC electric systems using superconducting”. 2017.
- [22] Manohar P, Ahmed W. “Superconducting fault current limiter to mitigate the effect of DC line fault in VSC-HVDC system”. *2012 Int. Conf. Power, Signals, Control. Comput.*, 1–6, 2012.
- [23] Xue S, Gao F, Sun W, Li B. “Protection principle for a DC distribution system with a resistive superconductive fault current limiter”. *Energies*, 8, 6, 4839–4852, 2015.

[24] Elmitwally A. “Proposed hybrid superconducting fault current limiter for distribution systems”. *Int. J. Electr. Power Energy Syst.*, 31, 10, 619–625, 2009.

[25] Langston J, Steurer M, Woodruff S, Baldwi T, Tang J. “A generic real-time computer simulation model for superconducting fault current limiters and its application in system protection studies”. *IEEE Trans. Appl. Supercond.*, 15, 2 PART II, 2090–2093, 2005.

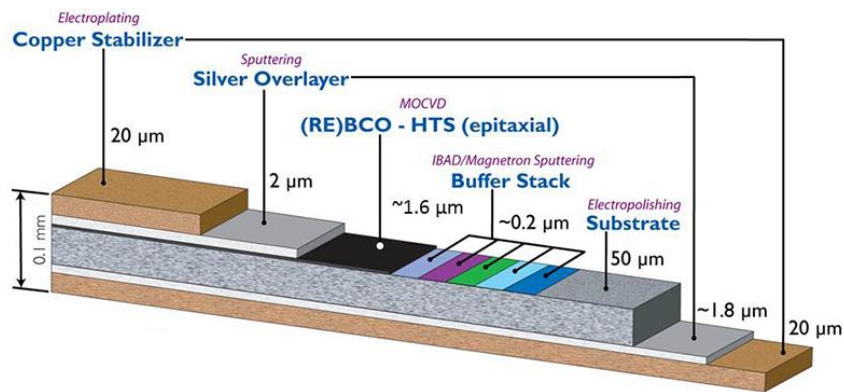
[26] Zhu J, Chen S, Jin Z. “Progress on second-generation high-temperature superconductor tape targeting resistive fault current limiter application”. *Electron.*, 11, 3, 2022.

[27] Escamez G, Vialle J, Bruzek CE, Grose V, Bauer M, Tixador P. “Numerical investigations of ReBCO conductors with high limitation electric field for HVDC SFCL”. *IEEE Trans. Appl. Supercond.*, 28, 4, 2018.

[28] Badel A, Escamez G, Tixador P. “REBCO FCL modelling: Influence of local critical current non-uniformities on overall behavior for various tape architectures”. *IEEE Trans. Appl. Supercond.*, 25, 3, 13–16, 2015.

Appendix A

Tape Structure



Tape Properties

	Minimum I_c measured by continuous direct current	Width	Total Wire Thickness	Critical Axial Tensile Strain at 77K	Critical Bend Diameter in Tension (40μm) @ room temp	Critical Bend Diameter in Compression (40μm) @ room temp
SCS6050	150 amp	6 mm	0.1 mm	0.45%	11 mm	11 mm